Original Article

DOI: 10.5582/bst.2019.01070

Conserved amino acids around the DIII-DI linker region of the Newcastle disease virus fusion protein are critical for protein folding and fusion activity

Miaomiao Chi[1], Wenyan Xie[2], Ying Liu[1], Chi Zhang[1], Yaqing Liu[1], Hongling Wen[1], Li Zhao[1], Yanyan Song[1], Na Liu[1], Lianli Chi[3], Zhiyu Wang[1,4,*]

[1] *Department of Virology, School of Public Health, Shandong University, Ji'nan, Shandong, China;*
[2] *Department of Laboratory Medicine, Shandong Provincial Qianfoshan Hospital, Shandong University, Ji'nan, Shandong, China;*
[3] *State Key Laboratory of Microbial Technology, National Glycoengineering Research Center, Shandong University, Ji'nan, Shandong, China;*
[4] *The Key Laboratory for Experimental Teratology of the Ministry of Education, Shandong University, Ji'nan, Shandong, China.*

Summary **Newcastle disease virus (NDV), an avian paramyxovirus, causes Newcastle disease (ND) which is a highly contagious and fatal viral disease affecting poultry and most species of birds. The fusion (F) protein of NDV mediates membrane fusion, which is essential to the processes of viral entry, replication, and dissemination. Although several domains of NDV F are known to have important effects on regulating the membrane fusion activity, the role of the region around domain III (DIII) and domain I (DI) still remains ill-defined. Site-directed mutagenesis was utilized to change the conserved amino acids at 269, 274, 277, 286, 287, 290, 295, and 297 to alanine in order to investigate the effects of these conserved amino acids around the DIII and DI linker region of the NDV F protein on fusion activity. It was found that five of these substitutions almost abolished fusion activity except for mutants I269A, Q286A, and N297A, which showed 57.1%, 161.1%, and 97.7% of the wt F level, respectively. Four (I274A, D277A, V287A, and P290A) of these five mutants likely result in interfering with folding or transporting of the molecule since these proteins were minimally expressed at the cell surface, formed aggregates, or not proteolytically cleaved. However, mutant L295A almost abolished fusion activity even with a similar level of cell surface expression. These data indicated that conserved amino acids around the DIII-DI linker region are critical for the folding of the F protein and have an important influence on fusion activity.**

Keywords: NDV, F protein, Membrane fusion, Protein folding and transport

1. Introduction

Newcastle disease virus (NDV) causes fatal infections in chicken (*1*), resulting in huge economic losses to the poultry industry. Current vaccination strategies are not fully efficacious and the development of new concepts for vaccine generation are needed since multiple outbreaks still occur worldwide (*2*) and NDV strains have been isolated from vaccinated chicken flocks (*1*). To develop new vaccines or therapeutic drugs, it is necessary to further clarify the fusion process caused by NDV.

Two viral surface glycoproteins, the hemagglutinin-neuraminidase (HN) protein and the fusion (F) protein, work together to accomplish the process of viral entry of NDV (*3,4*). HN glycoprotein is responsible for NDV's recognizing and binding to its target cells (*5*), whereas the F protein is the ultimate performer of membrane fusion, involved in the merger of the host-cell plasma membranes (*6,7*).

The NDV F protein, which belongs to type I integral membrane proteins (*8*), is initially synthesized as an inactive precursor, designated F_0, which is then

Released online in J-STAGE as advance publication May 28, 2019.

**Address correspondence to:*
Dr. Zhiyu Wang, Department of Virology, School of Public Health, Shandong University, Ji'nan 250012, Shandong, China.
E-mail: zhiyu.wang@sdu.edu.cn

activated by proteolytic cleavage into a hetero-dimer of F_1 and F_2 linked with a disulfide bridge during transport within the Golgi organelle (*9*). To achieve fusion with membrane, a hydrophobic amino acids stretch at the N-terminus of the F_1 subunit, named the 'fusion peptide' (FP) (Figure 1A), is released and inserted into the host cell membrane to initiate the fusion process. Then, two heptad repeat (HR) regions in the F_1 polypeptide, HRA (located at the C-terminal of the fusion peptide) and HRB (close to the trans-membrane region), fold onto each other to form a stable 6-helix bundle (6HB) that pulls the viral and target cell membranes together (*10-12*).

There is still a large intervening region with important functions between HRA and HRB (*9*), and current crystallographic structures divide this region into three distinct domains (Figure 1A), domains I-III, from the N-terminus to the C-terminus (*13*). From the top view of the F protein of NDV and human parainfluenza virus 3 (hPIV3) (*13*), it was found that the key domains of the heads were roughly of the same shape, but there were some differences in the orientation. This difference in orientation may be attributed to the different arrangements of domains DI-III, which may be related to the different junction regions among these domains (*13*).

Though no obvious or direct linkage exits between domains DIII and DI (Figure 1A), several important amino acids have been found around this junction. The NDV F protein L289A mutation found by Sergel *et*

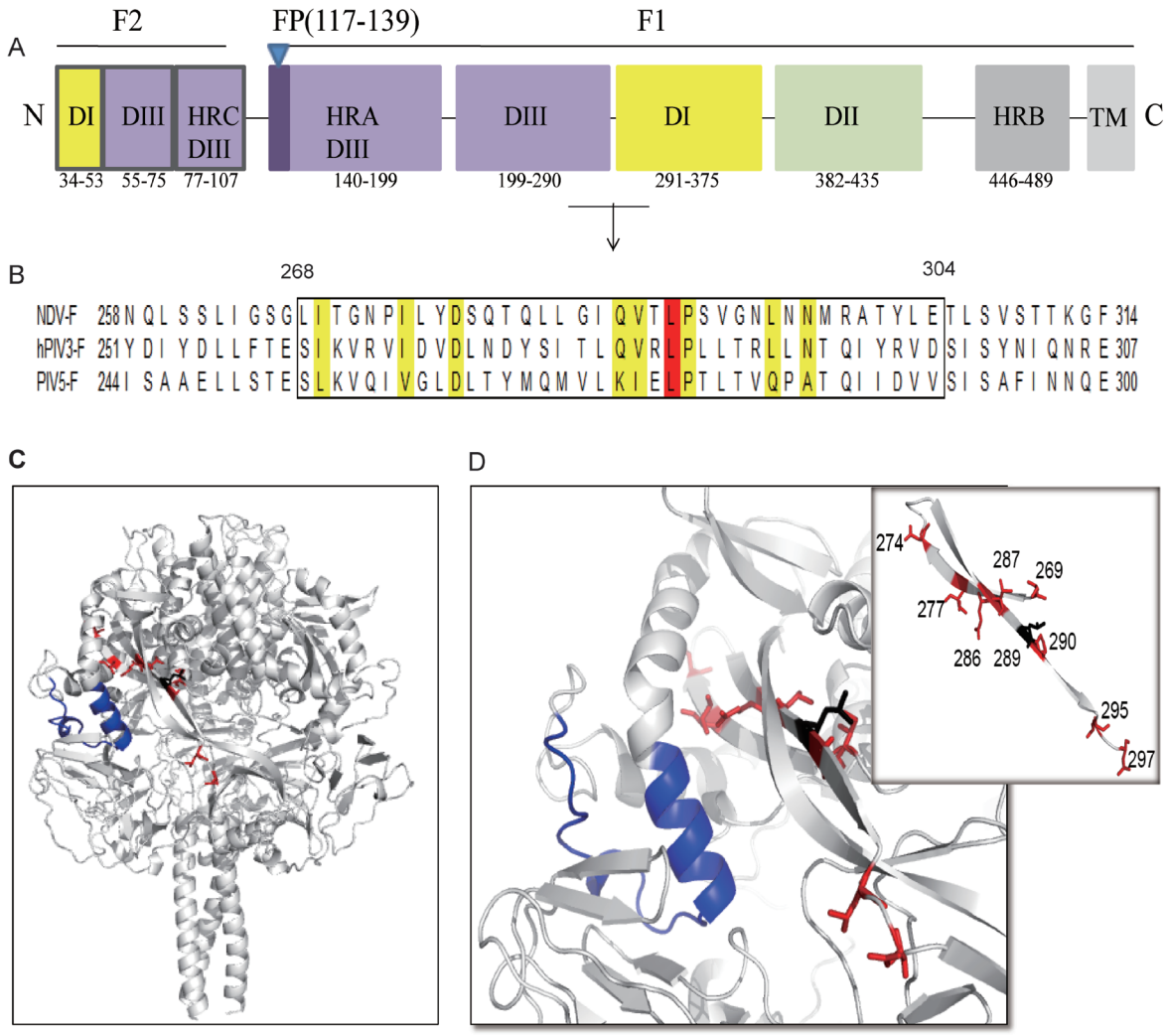

Figure 1. Schematic diagram of the locations of mutations. (A) Domain structure of the NDV F protein and the relative location of the DIII-DI junction in the primary sequence. Structural important domains are represented as different colors of rectangles, and their corresponding residue ranges are indicated below. Fusion peptide (FP), heptad repeat region (HR), and structural domains DI, DII, and DIII are shown. **(B)** Identification of the conserved amino acids around the DIII-DI linker region by sequence alignment using software MEGA 6.0. Residues in yellow = conserved amino acids for both NDV F and hPIV3, and residues in red show the position of the previously characterized hyperfusogenic mutant L289A. **(C)** Locations of the conserved amino acids in the pre-fusion NDV F protein homology modeling structure which was generated based on the crystal structure of the pre-fusion PIV5 F protein (PDB ID 2B9B). A side view of the ribbon diagram of the structural model of the NDV F protein in the pre-fusion conformation is shown. Three monomers are shown in white. The mutant residues are shown in stick mode in one chain, FP is highlighted as blue. **(D)** Close-up view of panel C, showing the conserved amino acids in cartoon and stick representation. Conserved amino acids are colored in red and labeled with site numbers. The known L289 site is colored in black. The figures were generated with PyMOL 0.99.

al. (*14*) can induce fusion without the HN protein. In addition, mutant L268A, which can attenuate F protein fusion, is also located around this region. Yin *et al*. (*13*) suggested an important site 304 in the NDV F protein around this region, corresponding to site 290 in parainfluenza virus 5 (PIV5) F, which is the determinant of the HN independent fusion induced by PIV5 F. Also, the amino acids of this segment are considered to be a key region that constitutes the radial channels (*15*) of the head of the F protein, which play an important role in the docking of FP.

Conserved sites were found around this junction region (peptide 268-304) by sequence alignment of the F protein from NDV, hPIV3, and PIV5 (Figure 1B), and we speculated that these amino acids were conserved due to important roles in the folding or fusion function of the F protein. To address this, mutational analysis of conserved amino acids between L268 and E304 was performed.

The alanine residue was introduced into sites I269, I274, D277, Q286, V287, P290, L295, and N297 with site-directed mutagenesis. The effects on the fusion activity, cell surface expression, and cleavage activity of each mutated F protein were examined. As a result, most of the mutants had a decreased fusogenic activity except for mutants Q286A and N297A. This decreased fusogenic activity may likely result from interfering with folding or transport of the molecule since most mutated proteins were minimally expressed at the cell surface. The results indicated that conserved amino acids around the DIII and DI junction are critical to the F protein's proper folding, transport, and membrane fusion activity.

2. Materials and Methods

2.1. *Homology modeling*

The structure of the NDV F protein in the pre-fusion conformation was generated based on the pre-fusion PIV5 F protein (*16*) (PDB ID 2B9B) on the SWISS-MODEL protein-modeling server (*17*). 2B9B was chosen as a template to generate the trimerical structure of NDV F because of its better coverage with NCBI Blast.

2.2. *Cell lines and viruses*

BHK-21cells, obtained from the American Type Culture Collection, were maintained in Dulbecco's modified Eagle's medium (DMEM) (Biological Industries (BI), Beit-Haemek, Israel) supplemented with 1% (v/v) glutamine, 10% (v/v) fetal calf serum (FCS) (BI), and 1% (v/v) penicillin-streptomycin (BI). The wild type (wt) vaccinia virus was used as a control to quantify cell fusion, while the recombinant vaccinia virus was used to provide the T7 RNA polymerase for the vaccinia-T7 RNA polymerase (vTF7-3) expression system.

2.3. *Site-directed mutagenesis*

Complementary oligonucleotide primers (Sangon Biotech Co. Ltd., Shanghai, China) with the appropriate sequence of the NDV F gene were designed to mutate these identified conserved amino acids. Overlapping PCR was used to produce each pair of the recombinant plasmids. Two products with a short homologous sequence were co-transformed into *Escherichia coli* DH5α cells, where they recombined to form a complete plasmid. All mutants were sequenced to verify that the mutations were successful.

2.4. *Syncytium formation assay*

BHK-21 cells were placed into 24-well plates 12 h before transfection. At 80% confluence, the cells were co-transfected with wt F or F mutant genes along with the NDV HN gene or the empty vector after incubation with the recombinant vaccinia virus 1h earlier at 37°C. At 24 h post transfection, monolayers were stained with Giemsa solution for syncytia observation under an inverted microscope (Olympus, Tokyo, Japan). Syncytia are cells with three or more nuclei.

2.5. *Content mixing assay*

To quantify the fusion activities mediated by different F mutants, a modified reporter gene assay was performed as previously described (*18,19*). Briefly, monolayers of BHK-21 cells infected with the recombinant vaccinia virus 1 h earlier at 37°C were co-transfected with the desired F and NDV HN genes. Monolayers of BHK-21 target cells infected with the wild-type vaccinia virus at a MOI of 10 1 h earlier at 37°C were transfected with 1 μg of plasmid pG1NT7 β-gal which encodes β-galactosidase. Following a 16 h incubation at 37°C, equal numbers (1×10^5) of the effector and target cells were combined in duplicate wells of a 96-well microtiter plate. After 7 h incubation at 37°C, the cells were assayed for β-galactosidase activity according to the procedures of the β-galactosidase assay kit (Beyotime Biotechnology, Shanghai, China). The level of fusion was quantified by subtracting background fusion of BHK-21 cells transfected with comparable amounts of the vector or only wt F.

2.6. *Dye transfer assay of lipid mixing*

The abilities of NDV F mutants and wt F to mediate lipid mixing were assessed by the transfer of octadecyl rhodamine b chloride (R18) (Invitrogen, California, USA) (*20*) from chicken red blood cells (RBCs) to BHK-21 cells co-transfected with NDV F and HN genes, using a modification of a protocol described by Bagai *et al*. (*21*). At 24 h post transfection, cell monolayers co-expressing the wt or mutated F and their

HN protein were washed and incubated with 50 mU/mL of neuraminidase (Sigma Chemical Co., St. Louis, Mo., USA) at 37°C for 1 h. Then the R18-labeled RBCs were added and incubated at 4°C for 30 min. Unbound RBCs were washed, and then the plate was incubated at 37°C for 1 h to initiate fusion. A fluorescent microscope (Olympus) was used to photograph the events of lipid mixing.

2.7. *Indirect immunofluorescence assay (IIFA)*

BHK-21cells were seeded into 24-well plates and transfected with wt F and F mutant genes. The monolayers were fixed with 4% paraformaldehyde after 24 h transfection, then incubated with anti-NDV antiserum (Abcam, Cambridge, UK) and a goat anti-chicken Alexa Fluor 488-conjugated immunoglobulin Y (H + L) (Abcam) was used as the secondary antibody. Photographs of the cells were taken under a fluorescent microscope (Olympus) after the secondary antibody was washed twice with cold PBS.

2.8. *Flow cytometry analysis*

Fluorescence-activated cell sorter (FACS) analysis was used to assay the cell surface expression of the wt F and each mutated F proteins as previously described (*22*). At 24 h post transfection, the monolayers were removed from plates by treatment with 5 mM EDTA in PBS, pelleted by centrifugation, washed twice, and blocked with PBSA (PBS with 3% bovine serum albumin) for 30 min on ice. The primary antibody and the secondary antibody were the same those as used in the IIFA assay. Then, the cells were fixed with 4% paraformaldehyde and re-suspended in 0.4 mL of PBSA for analysis with the CytoFLEX S Flow Cytometer (Beckman Coulter, Inc., California, USA). Cells transfected with only the vector were used as negative controls.

2.9. *Western blot (WB)*

To examine the cleavage activity of wt F and F mutants, BHK-21cells were transfected with wt F and F mutant plasmids using a standard transfection protocol. At 24 h post transfection, cell monolayers were removed from the 12-well plate by treatment with 50 mM EDTA in PBS, pelleted, and then lysed. Polypeptides were analyzed under a nonreducing condition using 10% SDS-PAGE without boiling. Anti-NDV antiserum recognizing the NDV F protein (Abcam) and an IRDye® 800CW donkey anti-chicken IgG (H + L) (LI-COR, Lincoln, Nebraska, USA) as the second antibody were used, and then the protein bands were scanned and visualized using Odyssey (LI-COR). To test for expression of D277A-His, an anti-His antibody (Proteintech, Wuhan, Hubei, China) and an IRDye® 800CW goat anti-mouse IgG (H + L) (LI-COR) were used.

2.10. *Statistical analysis*

All results were from at least three separate experiments and indicated as the mean ± SD. Statistical analysis was calculated by SPSS 17.0 using the Student's *t* test with a significance level of $p < 0.05$ (*), $p < 0.01$(**) and $p < 0.001$ (***), respectively.

3. Results

3.1. *Identification and mutagenesis of conserved amino acid residues around the DIII-DI linker region of the NDV F protein*

In order to identify the conserved amino acid residues around the DIII-DI linker region of the F protein, sequences from NDV, hPIV3, and PIV5 F proteins were aligned and analyzed. Eight conserved amino acid residues were found and site-directed mutagenesis was utilized to mutate to alanine at these sites (I269, I274, D277, Q286, V287, P290, L295, and N297) in order to determine the function for these conserved sites around the DIII-DI linker in the NDV F protein (Figure 1B).

The NDV F protein in the pre-fusion conformation was generated based on the pre-fusion PIV5 F protein (*16*) (PDB ID 2B9B) on the SWISS-MODEL protein-modeling server. These conserved sites were exhibited on the NDV F homology modeling structure (Figures 1C and 1D). Most of these sites were located within the F protein, while sites L295 and N297 were situated on the surface of this protein (Figure 1D).

3.2. *Fusion activity assessment for wt F and its mutants*

In order to explore the effects of these single amino acid substitutions of the conserved amino acids around the DIII-DI linker region of the NDV F protein on their fusogenic activity, three different types of membrane fusion assays were done.

The syncytium formation was initially observed to evaluate an overall level of cell-cell fusion. NDV wt or mutated F proteins were co-expressed in BHK-21 cells with their homologous HN protein. At 24 h post transfection, an inverted microscope was used to observe multinucleated giant cells and representative photomicrographs of syncytia are shown in Figure 2A. The cells expressing only the NDV wt F protein were used as negative controls. It was found that fewer syncytia were formed by mutant I269A compared with those produced by wt F and HN proteins. However, mutants I274A, P290A, and L295A had very limited ability to form syncytia and no syncytia were observed for mutants D277A and V287A. Only mutant Q286A produced significantly larger syncytia than wt F, while N297A did not affect the formation of syncytia. These results suggested that most of these mutants impaired the formation of syncytia except for mutants Q286A

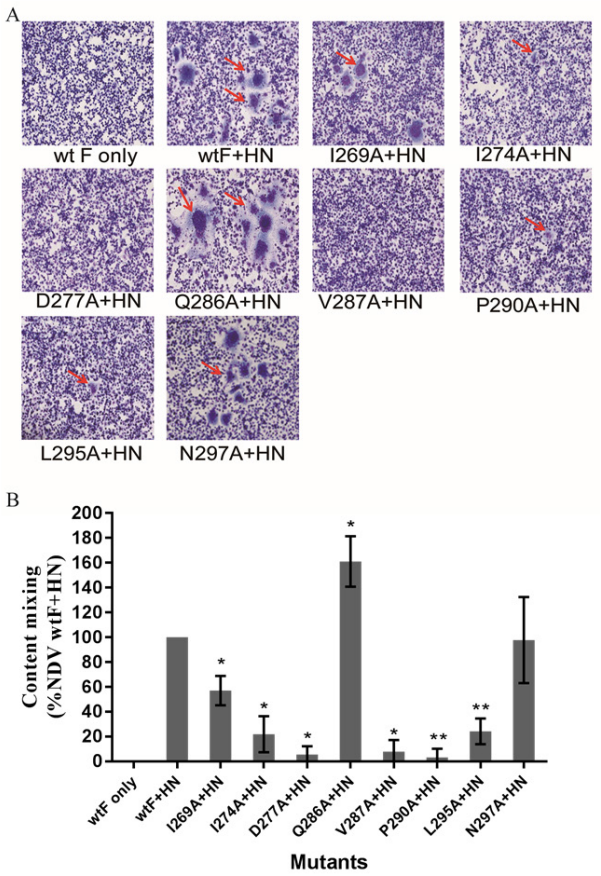

Figure 2. Syncytium formation and content mixing of NDV wt and mutated F proteins. (A) Syncytium formation in monolayers co-expressing wt or F mutant proteins and NDV HN. At 24 h post-transfection, BHK-21 monolayers transfected with only wt F, wt F and HN, or F mutants and HN were fixed with methanol and stained with Giemsa solution. Images were immediately acquired with a 10× objective under an inverted microscope. **(B)** Content mixing of wt F and F mutant proteins co-expressed with NDV HN. Values are expressed as percentages of content mixing detected in cells transfected with wt F and HN. The data represent the means of three independent experiments plus standard deviations. *P* values were calculated using the Student's *t* test to determine statistical significance of differences between each mutated F and wt F. (*, $p < 0.05$; **, $p < 0.01$; otherwise, $p > 0.05$)

and N297A.

To quantify the fusogenicity of these F mutations, a modification of the reporter gene assay was carried out to measure content mixing. Two populations of cells are indispensable for this assay: BHK-21 effector cells and BHK-21 target cells. Values were expressed as percentages of content mixing detected in cells transfected with wt F and HN proteins. The data are summarized in Figure 2B and Table 1. The F protein carrying the individual I269A mutation resulted in weakened content mixing, retaining only 57.1% of the wt F level, when co-expressed with the NDV HN protein. Mutants I274A and L295A reduced the levels of content mixing to extremely lower levels, 21.9% and 24.2% of that of wt F proteins. Additionally, a background level of fusion activity, 5.6%, 7.8%, and 3.0% of wt F, respectively, was detected for mutants

Table1. Functional profile of mutants around the DIII-I linker of NDV F (%wt F)

Name	Cell fusion (% of wt)	Cell surface expression (CSE)
wt F	100	100
I269A	57.1 ± 11.8	30.1 ± 3.8
I274A	21.9 ± 14.5	#
D277A	5.6 ± 6.7	#
Q286A	161.1 ± 20.3	94 ± 26.2
V287A	7.8 ± 9.4	#
P290A	3.0 ± 6.9	31.5 ± 19
L295A	24.2 ± 10.3	100 ± 21.6
N297A	97.7 ± 34.6	86.8 ± 23.9

The average of cell surface expression and cell fusion were determined with FACS and Report Gene Method, respectively. The data are averages of three independent experiments. Values are expressed as percentages of wt F. # means no detectable data.

D277A, V287A, and P290A. Mutant Q286A produced fusion activity over 1.5 fold of the level of the wt F, whereas mutant N297A showed a similar amount of fusion, approximately 97.7% of the wt F ($p > 0.05$). Therefore, most of the mutated F proteins led to reduction in content mixing except for Q286A and N297A, reflecting the results observed in the syncytial assay in Figure 2A.

Through the process of membrane fusion, activation of F and insertion of the FP into the target membrane initially led to the merger of the lipid bilayers before fusion pore formation and content mixing (*23*). To address whether or not the mutated F proteins impaired their ability to mediate lipid mixing, a dye transfer assay with R18-labeled RBCs was carried out to assess the extent of the lipophilic probe R18 transfer from RBC membranes to transfected BHK-21 cell membranes. Two negative controls were set for this experiment: cells expressing only NDV HN and only the F protein. As expected, cells expressing the HN protein bound RBCs, but there was no transfer of fluorescence from the RBCs to the BHK-21 cells. In contrast, cells expressing both HN and wt F proteins became more fluorescent as a result of the dye transfer (Figure 3). The results of lipid mixing almost mirrored the Giemsa staining results of wt or mutated F and the HN protein. Five of these mutants (I274A, D277A, V287A, P290A, and L295A) produced only a very small number of fusion events, almost similar to the negative control level. In addition, mutant I269A showed less and weak fluorescence. However, mutant Q286A showed a stronger fluorescence than wt F, while mutant N297A produced a similar level in lipid mixing. Therefore, these alanine substitutions also resulted in defects in mediating lipid mixing except for Q286A and N297A.

3.3. *Cell surface expression of wt F and its mutants*

Indirect immunofluorescence detection of the F protein on the surfaces of intact cells transfected with mutant F

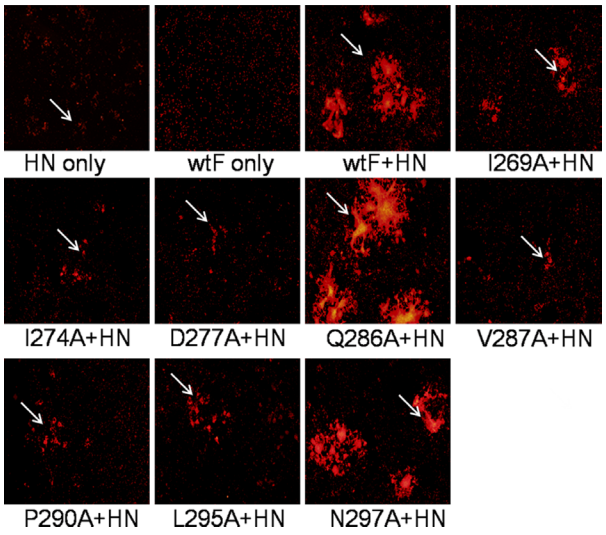

Figure 3. Promotion of lipid mixing for NDV wt and mutant F proteins. The extent of lipid mixing is shown by the spread of the dye transferred from R18-labeled red blood cells (RBCs) into the cell membranes of transfected BHK-21 cells. Labeled RBCs were added to each monolayer, and then the cells were incubated on ice for 30 min. After 30 min, the cells were washed and fusion between the transfected cells and RBCs was initiated by transferring the cells to 37°C for 1 h. Images were immediately acquired under a fluorescent microscope

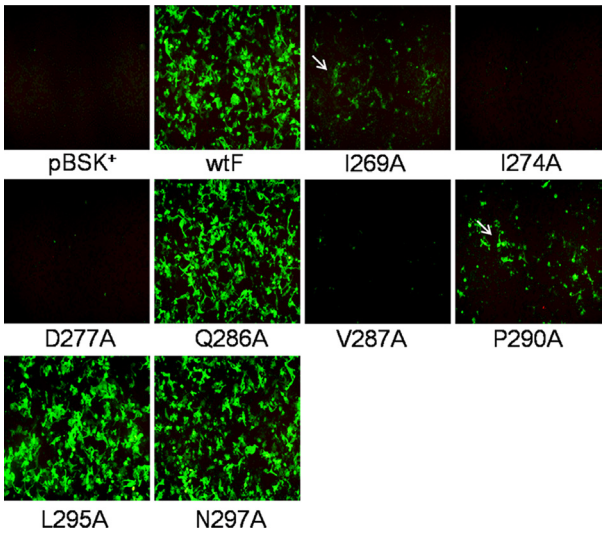

Figure 4. Expression of wt F and F mutant proteins detected with indirect immunofluorescent assay (IIFA). Intact confluent monolayers of BHK-21 cells transfected with wild-type or mutant F protein cDNAs were incubated with anti-NDV antiserum and then with fluorescent-labeled goat anti-chicken antibody. All fields shown were obtained using a 20× objective. White arrows indicate scattered fluorescent points.

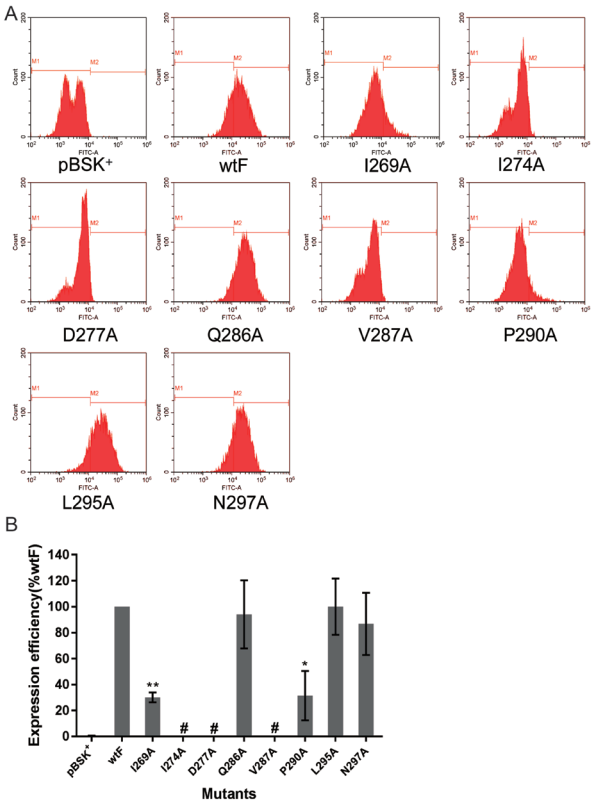

Figure 5. Quantitative expression of wt F and F mutant proteins detected with FACS analysis. Surface expression levels of wt F and F mutants were determined with FACS analysis at 24 h post-transfection using anti-NDV antiserum and then with fluorescent-labeled goat anti-chicken antibody, the same as used in the IIFA assay. **(A)** Representative fluorescent histograms for each mutant are shown. The x axis is the fluorescent intensity values shown in log scale and the y axis is cell counts. **(B)** Quantitation of the cell surface expression level detected by FACS analysis. Data were normalized to the value obtained with wt F. The means and standard errors are from triplicate experiments, # means no detectable data. (*, $p < 0.05$; **, $p < 0.01$; otherwise, $p > 0.05$).

protein genes was used to determine whether or not the mutant proteins were expressed at the cell surface. As shown in Figure 4, three of these F mutants (Q286A, L295A, and N297A) were detected at the surface, with a fluorescent signal similar to that of the wild-type protein. Mutant I269A and P290A were also detected at the surface, although the signal was much less intense than that of wt F. However, mutants I274A, D277A, and V287A were not detected at the cell surface.

Surface expressions of these mutants were quantitated with FACS analysis and compared with that of wt F. Mutants I274A, D277A, and V287A could not be detected with FACS, while mutants Q286A, L295A, and N297A were very well expressed, 94%, 100%, and 86.8% of that of wt F, respectively ($p > 0.05$). However, mutants I269A and P290A showed a reduced expression level, only about one-thirds of that of wt F (Figure 5 and Table 1).

3.4. *Cleavage activity of NDV wt F and mutants*

The cleavage abilities of the NDV wt F and mutants expressed in BHK-21 cells were detected with total cell lysates. The results from Western blot assay showed that mutants I274A, D277A, and V287A were non-cleaved and expressed less than the wt F protein (Figure 6). Mutants I269A, Q286A, P290A, L295A, and N297A showed similar cleavage efficiency. However, a high expression level in total cell lysate for P290A

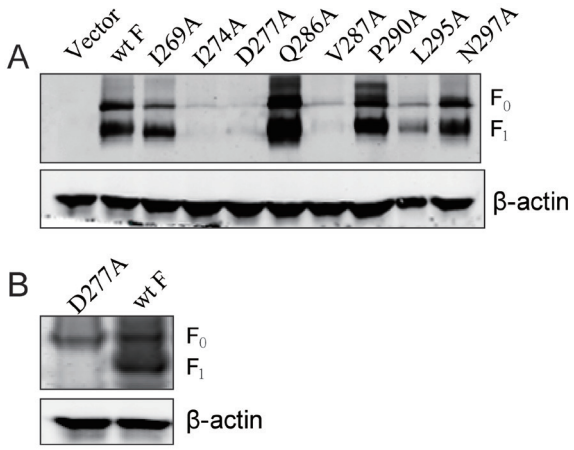

Figure 6. Expression and cleavage of NDV wt F and F mutants transfected without HN. At 24 h post-transfection, the wt F and F mutants transfected BHK-21cells were harvested and lysed. **(A)** Expression and cleavage of NDV F proteins from total cell lysates were detected using Western blot without boiling or reducing. **(B)** To detect total expression of D277A, a 6× His was introduced at C- terminal. The total cell lysates were detected with His tag antibody under a boiling and reducing condition. The positions of precursor (F_0) and cleaved subunit (F_1) of the F protein are shown.

was detected, which was contrary to its reduced cell surface expression levels detected with FACS. It is worth noting that an extra slower-migrating band than F_0 was detected for mutants Q286A and P290A, which may have been protein aggregates due to high level expression of whole protein molecules.

4. Discussion

F protein-mediated membrane fusion is an important process for NDV to complete cell invasion and dissemination. The exact steps of the F protein from a pre-fusion conformation to a post-fusion conformation during the fusion process are not fully understood, but biochemical and physiological evidences along with X-crystal structures outline how the F protein mediates viral and cell membrane fusion (*10,11,13,15,24-27*). The key conformational changes in the F-protein refolding pathway have been highlighted, including the insertion of FP (*25*) and the forming of 6HB (*10*). Through this process, DI-DIII domains rearranged their orientation or structure to help achieve fusion. DI and DII as rigid modules are repositioned during the conformational transition, while a refolding process occurs in DIII (*15,16*). In this condition, potential hinge points, especially the linker between domains I and III, could be important for potential structural and functional changes (*13*).

In the present study, eight conserved sites near the junction of domains DIII and DI were found and the impacts of these sites on protein expression and membrane fusion were assessed after site-directed mutagenesis. The results showed that the fusion activities of the majority of mutant proteins were reduced, among which three mutants (I274A, D277A, and V287A) completely lost fusion ability. However, Q286A exhibited an increased ability to mediate cell fusion and N297A performed a similar level of fusion compared with wt F.

The lost fusion ability was found to be closely related to undetected cell surface protein expression. Three mutants (I274A, D277A, and V287A), for example, were poorly expressed at the cell surface and as a result no fusion activities were detected. Only a weak F_0 band was detected by anti-NDV antiserum. This reduction in expression may be attributed to the abnormal structure since the anti-NDV antiserum only recognizes natural NDV F trimers. To further detect expression of D277A (an example of the mutants undetectable with NDV antiserum), a 6× His tag was introduced at the C-terminal and a reducing WB was carried out. The results showed that D277A displayed a single F_0 band without F_1 compared with wt F. Thus, this lost fusion capability of these three mutants (I274A, D277A, and V287A) may directly correlate with the non-cleavage of the F protein. Interestingly, these three mutants were present within the structure of NDV F (Figure 1D), suggesting important roles of these inside amino acids in protein folding. As expected, mutant I269A and P290A, which are located inside the F protein, also showed a reduced surface expression level, with only about 30% of that of wt F. However, these kinds of reduced surface expression were different from those of I274A, D277A, and V287A, which may result from defects in transport to the cell surface (Figures 4 and 6). Mutant P290A showed an impaired expression on the cell surface but a higher level in total protein expression than wt F (Figure 6A). This indicated that the P290A protein may accumulate within the cell cytoplasm and cannot be properly transported to the cell membrane (*9*). However, another inside site, mutant Q286A produced an F protein, which exhibited a hyperfusogenic phenotype in our study. A similar inside site, like L289A (Figure 1D, colored as black), was reported to increase the fusion activity or even induce HN independent fusion (*14*). However, Q286A did not induce the same HN-independent fusion as L289A in our study, while it expressed in BHK-21 cells alone (Data not shown). Whether or not the Q286A mutant could induce fusion without HN needs to be further tested in more cell lines, since the HN-independent fusion of L289A is cell-specific (*28*). Two mutants, T458D and G459D, in the linker between domain I and HRB of NDV F are proved to increase fusion activity and induce HN independent fusion regardless of cell types (*22*). Our results along with these results suggested important roles of the connecting region between different domains in regulating the fusion activity of the NDV F protein.

A special site was mutant L295A, which almost lost fusion activity with a similar level of cell surface

expression. Shown as the generated pre-fusion form of the NDV F protein (Figure 1D), this amino acid was located on the surface of the protein molecule. Thus, a possible explanation is that this mutant may have an influence on the interaction between HN and F (*24*). In addition, mutant N297A was another site located on the surface of the protein structure (Figure 1D) without affecting expression. However, N297A had a similar level of fusion to wt F. The different levels of fusion activity for these two surface amino acids indicated that a hydrophobic amino acid is more likely to participate in the interaction between HN and F (*24*). Thus, site L295 could be a potential drug target to block the interplay between HN and F by a mimic peptide (*29*) with the sequence surrounding this site.

In the NDV F protein, the above conserved sites are located within or near the radial channels (*14,15*). The radial channels are considered to be the "dock" of the FP (*13,15*), which plays an important role in the correct insertion of the FP into the host cell membrane. Thus, these sites may be important in maintaining the correct structure of radial channels and mutations of these sites could influence the intrinsic radial channels, resulting in defects in the protein structure. A more detailed description of the refolding process of PIV5 F found that two peptides, 239-272 and 273-308, showed significant changes in oxidation states during the release of FP (*25*). These two peptides correspond to peptides 250-283 and 284-319, respectively, of the NDV F, which is the area surrounding the DIII-DI (peptide 268-304) junction. Thus, conservative amino acid mutant introduction may destroy the relative activities of these two fragments, affecting the fusion process F proteins. Given that the DIII-DI connection region appears to be a conserved structure in paramyxovirus F proteins, this region presents an alternative way to investigate structure-based rational vaccine or drug designs (*30,31*).

In conclusion, this study identified eight conserved amino acids at the junction of domains DIII and DI, seven of which play important roles in the folding, transport and regulation of the F protein's fusion activity. However, different sites play different roles. For example, sites I274, D277, and V287 are important for F's folding and cleavage activation. And two other sites, I269 and P290, are essential for protein transport. In addition, site L295 may participate in the interaction between HN and F. A deeper understanding of the roles of this junction region in the structure and function of the F protein could lay the foundation for developing new structure-based antiviral vaccines or drugs.

Acknowledgements

We gratefully thank Dr. Ronald M. Iorio for providing the recombinant plasmid vectors and Dr. Bernard Moss for the recombinant vaccinia virus, vTF7-3. This work was supported by grants from National Natural Science Foundation of China (No.81672011; No.81271806) and the Fundamental Research Funds of Shandong University (2015JC044). Thanks to Dr. Edward C. Mignot, Shandong University, for linguistic advice.

References

1. Zhu J, Hu S, Xu H, Liu J, Zhao Z, Wang X, Liu X. Characterization of virulent Newcastle disease viruses from vaccinated chicken flocks in Eastern China. BMC Vet Res. 2016; 12:113.
2. Dimitrov KM, Afonso CL, Yu Q, Miller PJ. Newcastle disease vaccines-A solved problem or a continuous challenge? Vet Microbiol. 2017; 206:126-136.
3. Paterson RG, Johnson ML, Lamb RA. Paramyxovirus fusion (F) protein and hemagglutinin-neuraminidase (HN) protein interactions: Intracellular retention of F and HN does not affect transport of the homotypic HN or F protein. Virology. 1997; 237:1-9.
4. Tong S, Compans RW. Alternative mechanisms of interaction between homotypic and heterotypic parainfluenza virus HN and F proteins. J Gen Virol. 1999; 80:107-115.
5. Iorio RM, Syddall RJ, Sheehan JP, Bratt MA, Glickman RL, Riel AM. Neutralization map of the hemagglutinin-neuraminidase glycoprotein of Newcastle disease virus: Domains recognized by monoclonal antibodies that prevent receptor recognition. J Virol. 1991; 65:4999-5006.
6. Dutch RE, Jardetzky TS, Lamb RA. Virus Membrane Fusion Proteins: Biological Machines that Undergo a Metamorphosis. Biosci Rep. 2000; 20:597-612.
7. Weissenhorn W, Hinz A, Gaudin Y. Virus membrane fusion. FEBS Lett. 2007; 581:2150-2155.
8. White JM, Delos SE, Brecher M, Schornberg K. Structures and mechanisms of viral membrane fusion proteins: Multiple variations on a common theme. Crit Rev Biochem Mol Biol. 2008; 43:189-219.
9. Gardner AE, Martin KL, Dutch RE. A conserved region between the heptad repeats of paramyxovirus fusion proteins is critical for proper F protein folding. Biochemistry. 2007; 46:5094-5105.
10. Yu M, Wang E, Liu Y, Cao D, Jin N, Zhang CW, Bartlam M, Rao Z, Tien P, Gao GF. Six-helix bundle assembly and characterization of heptad repeat regions from the F protein of Newcastle disease virus. J Gen Virol. 2002; 83:623-629.
11. Baker KA, Dutch RE, Lamb RA, Jardetzky TS. Structural basis for paramyxovirus-mediated membrane fusion. Mol Cell. 1999; 3:309-319.
12. Epand RM. Fusion peptides and the mechanism of viral fusion. Biochim Biophys Acta. 2003; 1614:116-121.
13. Yin HS, Paterson RG, Wen X, Lamb RA, Jardetzky TS. Structure of the uncleaved ectodomain of the paramyxovirus (hPIV3) fusion protein. Proc Natl Acad Sci U S A. 2005; 102:9288-9293.
14. Sergel TA, McGinnes LW, Morrison TG. A single amino acid change in the Newcastle disease virus fusion protein alters the requirement for HN protein in fusion. J Virol. 2000; 74:5101-5107.
15. Chen L, Gorman JJ, McKimm-Breschkin J, Lawrence LJ, Tulloch PA, Smith BJ, Colman PM, Lawrence MC. The structure of the fusion glycoprotein of Newcastle disease virus suggests a novel paradigm for the molecular

mechanism of membrane fusion. Structure. 2001; 9:255-266.
16. Yin HS, Wen X, Paterson RG, Lamb RA, Jardetzky TS. Structure of the parainfluenza virus 5 F protein in its metastable, prefusion conformation. Nature. 2006; 439:38-44.
17. Waterhouse A, Bertoni M, Bienert S, Studer G, Tauriello G, Gumienny R, Heer FT, de Beer TAP, Rempfer C, Bordoli L, Lepore R, Schwede T. SWISS-MODEL: homology modelling of protein structures and complexes. Nucleic Acids Res. 2018; 46:W296-w303.
18. Navaratnarajah CK, Oezguen N, Rupp L, Kay L, Leonard VH, Braun W, Cattaneo R. The heads of the measles virus attachment protein move to transmit the fusion-triggering signal. Nat Struct Mol Biol. 2011; 18:128-134.
19. Jardetzky TS, Lamb RA. Activation of paramyxovirus membrane fusion and virus entry. Curr Opin Virol. 2014; 1:24-33.
20. Blumenthal R, Gallo SA, Viard M, Raviv Y, Dri M, Puri A. Fluorescent lipid probes in the study of viral membrane fusion. Chem Phys Lipids. 2002; 116:39-55.
21. Bagai S, Lamb RA. Quantitative measurement of paramyxovirus fusion: differences in requirements of glycoproteins between simian virus 5 and human parainfluenza virus 3 or Newcastle disease virus. J Virol. 1995; 69:6712-6719.
22. Ji Y, Liu T, Jia Y, Liu B, Yu Q, Cui X, Guo F, Chang H, Zhu Q. Two single mutations in the fusion protein of Newcastle disease virus confer hemagglutinin-neuraminidase independent fusion promotion and attenuate the pathogenicity in chickens. Virology. 2017; 509:146-151.
23. Russell CJ, Kantor KL, Jardetzky TS, Lamb RA. A dual-functional paramyxovirus F protein regulatory switch segment: activation and membrane fusion. J Cell Biol. 2003; 163:363-374.
24. Bose S, Heath CM, Shah PA, Alayyoubi M, Jardetzky TS, Lamb RA. Mutations in the parainfluenza virus 5 fusion protein reveal domains important for fusion triggering and metastability. J Virol. 2013; 87:13520-13531.
25. Poor TA, Jones L, Sood A, Leser GP, Plasencia MD, Rempel DL, Jardetzky TS, Woods RJ, Gross ML, Lamb RA. Probing the paramyxovirus fusion (F) protein-refolding event from pre- to postfusion by oxidative footprinting. Proc Natl Acad Sci USA. 2014; 111:E2596-E2605.
26. Welch BD, Liu Y, Kors CA, Leser GP, Jardetzky TS, Lamb RA. Structure of the cleavage-activated prefusion form of the parainfluenza virus 5 fusion protein. Proc Nat Acad Sci USA. 2012; 109:16672-16677.
27. Swanson K, Wen X, Leser GP, Paterson RG, Lamb RA, Jardetzky TS. Structure of the Newcastle disease virus F protein in the post-fusion conformation. Virology. 2010; 402:372-379.
28. Li J, Melanson VR, Mirza AM, Iorio RM. Decreased dependence on receptor recognition for the fusion promotion activity of L289A-mutated newcastle disease virus fusion protein correlates with a monoclonal antibody-detected conformational change. J Virol. 2005; 79:1180-1190.
29. Young JK, Li D, Abramowitz MC, Morrison TG. Interaction of peptides with sequences from the Newcastle disease virus fusion protein heptad repeat regions. J Virol. 1999; 73:5945-5956.
30. Song AS, Poor TA, Abriata LA, Jardetzky TS, Dal Peraro M, Lamb RA. Immobilization of the N-terminal helix stabilizes prefusion paramyxovirus fusion proteins. Proc Natl Acad Sci U S A. 2016; 113:E3844-3851.
31. Stewart-Jones GBE, Chuang GY, Xu K, *et al*. Structure-based design of a quadrivalent fusion glycoprotein vaccine for human parainfluenza virus types 1-4. Proc Natl Acad Sci U S A. 2018; 115:12265-12270.

(Received March 17, 2019; Revised April 21, 2019; Accepted May 17, 2019)